Iterative properties of a one-dimensional quartic map: Critical lines and tricritical behavior

Shau-Jin Chang, Michael Wortis, and Jon A. Wright
Department of Physics, University of Illinois at Urbana-Champaign, 1110 West Green Street, Urbana, Illinois 61801
(Received 13 July 1981)

This paper studies the iterative properties of the two-parameter family of maps $x_{n+1} = 1 + ax_n^2 + bx_n^4$. These maps can have either one or three extrema. Multiple extrema lead to a complex region of iterative stability and to new types of iterative behavior. In particular, the Feigenbaum critical line (locus of 2^n-cycle accumulations) present for $b \simeq 0$ terminates at two tricritical points T and T' with coordinates $(a,b) = (0, -1.594\,90)$ and $(-2.814\,03, 1.407\,01)$, respectively. There is also a "dual" critical line terminating in two additional tricritical points $\tilde{T} = (-3.189\,80, 2.543\,71)$ and $\tilde{T}' = (0.955\,61, -1.149\,81)$. Behavior near the tricritical points is controlled by a new fixed point f_T^* of the functional recursion relation $f_{n+1}(x) = [1/f_n(1)]f^{(2)}(xf_n(1))$. This fixed point has two relevant directions and, therefore, behavior near a tricritical point depends on two new universal numbers $\delta_T^{(1)} = 7.284\,69$ and $\delta_T^{(2)} = 2.857\,13$. Crossover and scaling behavior near the tricritical points are explored.

I. INTRODUCTION

Iterative properties $x_{n+1} = f(x_n)$ of one-dimensional continuous maps provide what is probably the simplest examples of nonlinear dissipative dynamical behavior and have attracted considerable attention in recent years.[1,2] Changing a single control parameter in such maps may lead from stable fixed-point behavior via a sequence of bifurcations to chaotic or quasichaotic behavior. Feigenbaum[3] showed that the limiting form of such bifurcation sequences exhibited scaling properties characterized by universal numbers, in strict analogy to critical behavior in statistical mechanics, and indeed, that the renormalization-group ideas developed in the statistical-mechanics context[4] could be fruitfully carried over. Such bifurcation sequences are also seen in higher-dimensional models[1,5,6] and in experiments.[7] They represent one possible kind of "transition to chaos." Feigenbaum's universal numbers have, in fact, cropped up in some higher-dimensional systems.[7]

The prototypical one-dimensional map is the so-called logistic map,

$$f(x) = \lambda x(1-x), \tag{1.1}$$

which for $0 \leq \lambda \leq 4$ maps the unit interval $[0,1]$ onto itself. Equation (1.1) is equivalent under change of origin and rescaling to the symmetric quadratic map,[8]

$$f(x) = 1 + ax^2. \tag{1.2}$$

In particular, the main bifurcation sequence has its limit at $a_c = -1.401\,16$. There is[1] a simple sequence of 2^n cycles for $a_c < a \leq \frac{1}{4}$ and a corresponding inverse-bifurcation sequence of more complicated 2^n bands[9] for $-2 \leq a < a_c$. The vicinity of the point a_c is characterized by a scaling behavior.[3] For example, the position a_n of the superstable 2^n cycle for $a > a_c$ and large n varies as

$$a_n - a_c = A/\delta_F^n, \tag{1.3}$$

where $\delta_F = 4.669\,20$ is one of Feigenbaum's universal "critial exponents" and the nonuniversal amplitude $A = 9.349$. (The actual exponents in statistical mechanics are really related to $\ln\delta_F$.) So far, we have discussed only the logistic map (1.2). It is known, however, that the behavior of the logistic map provides a precise model for a large class[10] of single-peak functions: The ordering of n cycles[11] and the critical behavior[3,12] are universal; only the nonuniversal constants a_c and A vary from map to map.

It is the purpose of this paper[13] to study the behavior of a simple two-parameter class of maps which includes (1.2), the symmetric quartic maps,

$$f(x) = 1 + ax^2 + bx^4. \tag{1.4}$$

The distinctive feature of the maps (1.4) is that for $ab < 0$ they have three extrema, at

$$x_0 = 0, \quad x_\pm = \pm\sqrt{-a/2b}, \tag{1.5}$$

rather than one as (1.2). This multiple-peak or multiple-valley structure makes possible a plethora of new, interesting, and complicated iterative behavior. It is the purpose of this paper to survey in a partially empirical and certainly nonrigorous way some of the new behavior in the context of the two-parameter family (1.4).

Section II of the paper treats general, noncritical properties. In the one-extremum regions ($ab > 0$) behavior like that of the logistic map is observed, only the accumulation point a_c is drawn out into a "critical line." This critical line terminates in the regions $ab \leq 0$, where it is "pinched off" at tricritical points T and T' by the existence of behavior more complicated than a monotonic cascade of 2^n-cycle regions. When $ab < 0$, it is quite possible for two stable cycles (but apparently no more than two) to coexist. Superstable cycles

must pass through one of the extrema (1.5). For special values of (a,b) a single "doubly stable" cycle may use two of them. Tricritical points are associated with $n \to \infty$ limits of doubly stable 2^n cycles.

We develop a special form of topological conjugacy, called duality. Dual points P and $\tilde{P}$ have the same iterative properties. The dual of the critical line TT' is another critical line $\tilde{T}\tilde{T}'$ in the a,b plane.

We determine the region of the a,b plane over which the function (1.4) is iteratively stable, i.e., possesses a set of points x of nonzero measure with bounded itineraries.

Section III is devoted to the special properties of the map (1.4) near the endpoints T and T' of the critical line. Feigenbaum[3] showed that the points on the critical line were associated with a fixed point of a certain functional recursion relation. The tricritical points T and T' are associated with a different fixed point of the same functional recursion relation. At this new fixed point there are two relevant directions and, therefore, two new universal numbers.

We discuss the scaling properties of the regions near the tricritical points and the crossover behavior between critical and tricritical regimes. The fixed points associated with $\tilde{T}\tilde{T}'$ are different from those associated with TT' but related to them by topological conjugacy.

II. GENERAL PROPERTIES UNDER ITERATION OF THE SYMMETRIC QUARTIC MAP

This section describes certain general, noncritical properties of the map (1.4).

A. Preliminaries

The possible shapes of the symmetric quartic map (1.4) depend on the relative signs and magnitudes of the parameters a and b, as shown in Fig. 1. The curves have one local extremum in quadrants I and III and three in quadrants II and IV. The number of intersections of $y=f(x)$ with the straight line $y=x$ may be zero, two, or four. The regions of each behavior are indicated in Fig. 1 and the corresponding curves are sketched in Fig. 2.

Itineraries $x \equiv x_1, x_2(x), x_3(x), \ldots$ of an initial point x under iteration (1.4) are of several types.[2] We refer to as *bounded* those itineraries such that $|x_n| \not\to \infty$ as $n \to \infty$. Itineraries such that $|x_n| \to \infty$ as $n \to \infty$ are *unbounded*. The set of x having bounded itineraries is the *iterative domain* of f. When the iterative domain of f has nonzero measure, then f is *iteratively stable*, otherwise, it is *iteratively unstable*. We wish to explore in the

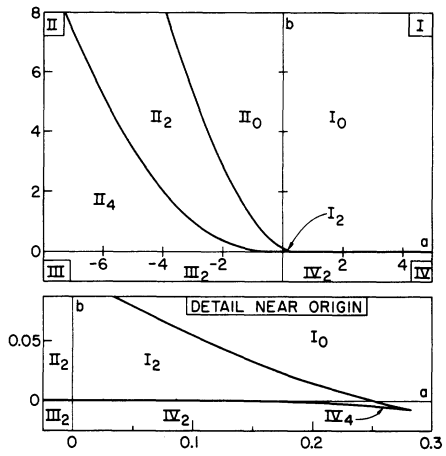

FIG. 1. Four quadrants of the a,b plane, indicating the number of intersections of $y=1+ax^2+bx^4$ with $y=x$. Detail shows region near the origin. Note that there is a small region of quadrant I where there are two intersections and an even smaller region of quadrant IV where there are four. Corresponding curves are sketched in Fig. 2.

remainder of this section the character and extent of the iterative domain of the map (1.4) for various values of the parameters a and b.

We distinguish the following types of bounded itineraries: (a) fixed points and other n cycles, (b) itineraries which, as $n \to \infty$, approach (are attracted by) a fixed point or other n cycle, and (c) other bounded itineraries, which we call *chaotic*.[14] The set of n cycles corresponds to the set of solutions of

$$x = f^{(n)}(x), \tag{2.1}$$

where we have denoted $f^{(n)} \equiv f \circ f \circ f \circ \cdots \circ f$ and $f \circ g(x) \equiv f(g(x))$. This set is countable and, therefore, contributes in and of itself zero measure to the iterative domain of f. The n cycle $x_1, x_2, \ldots, x_n, x_{n+1} \equiv x_1$ is *stable*, if a finite region of nearby x's is attracted to it, otherwise, it is *unstable*.

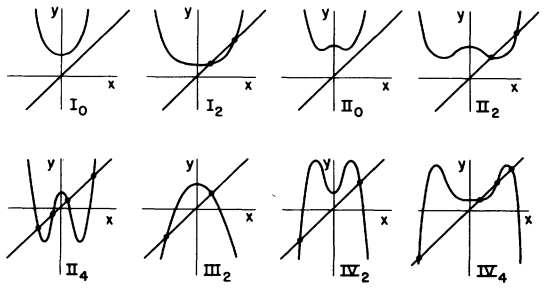

FIG. 2. Sketched shapes of the curve $y=1+ax^2+bx^4$ in the various regions of the a,b plane shown in Fig. 1. Intersections with $y=x$ are shown.

In particular, it is stable (unstable) if

$$\left|\frac{d}{dx_1} f^{(n)}(x_1)\right| < 1 \ (>1). \tag{2.2}$$

When

$$\frac{d}{dx_1} f^{(n)}(x_1) = 0, \tag{2.3}$$

the n cycle is *superstable*.[15] A function f is iteratively stable if and only if it has one or more stable n cycles and/or a domain of x's of nonzero measure with chaotic itineraries.

When f is iteratively stable, we shall wish to distinguish the number of different types of (bounded) limiting behavior occurring in the iterative domain of f. If all x's except for a set of measure zero have the same limiting behavior (e.g., if all are attracted to a single stable n cycle or if all have chaotic itineraries using the same domain), then f is *unimodal*[16]; if two distinct types of limiting behavior occur with nonzero measure, then f is *bimodal*, and so forth.

B. Topological conjugacy duality

It is useful before proceeding further to establish two important symmetry properties. Let h be an arbitrary locally invertible map and define

$$g \equiv h^{-1} \circ f \circ h, \tag{2.4}$$

so $f = h \circ g \circ h^{-1}$. Maps f and g related by (2.4) are called *topologically conjugate*.[2,11] Itineraries of f and g are related to one another in a simple one-to-one manner: any bounded (unbounded) itinerary of f maps into a bounded (unbounded) itinerary of g and conversely. Map g is iteratively stable if and only if f is. Similarly, n cycles map to n cycles, chaotic itineraries to chaotic itineraries, etc.

For general h the functional forms of the topologically conjugate maps f and g will be quite different. Two instances when this is not so are translations,

$$h_T(a,x) \equiv x - a, \quad h_T^{-1}(a,x) = x + a, \tag{2.5}$$

and scale changes,

$$h_S(a,x) \equiv ax, \quad h_S^{-1}(a,x) = x/a, \tag{2.6}$$

both of which take nth degree polynomials into nth degree polynomials. For example, the general symmetric quartic polynomial ($C \neq 0$)

$$F(x) = C + Ax^2 + Bx^4 \tag{2.7}$$

is topologically conjugate under scale change to the standard, normalized form (1.4), with $a = AC$, $b = BC^3$ via

$$f = h_S^{-1}(C) \circ F \circ h_S(C), \tag{2.8}$$

since

$$F(x) = C\left[1 + AC\left(\frac{x}{C}\right)^2 + BC^3\left(\frac{x}{C}\right)^4\right]. \tag{2.9}$$

There is a special form of topological conjugacy which is exceedingly valuable in studying the iterative properties of the quartic map (1.4). Note that

$$f(x) = 1 - \frac{a^2}{4b} + b\left(\frac{a}{2b} + x^2\right)^2 = G_1(G_2(x)), \tag{2.10}$$

with

$$G_1(x) = 1 - \frac{a^2}{4b} + bx^2$$

and

$$G_2(x) = \frac{a}{2b} + x^2. \tag{2.11}$$

Because $G_2 \circ G_1 = G_1^{-1} \circ (G_1 \circ G_2) \circ G_1$, f is topologically conjugate to the map $G_2 \circ G_1$ and, therefore, through (2.8) to the normalized map

$$\tilde{f} = h_S^{-1}(d) \circ G_2 \circ G_1 \circ h_S(d), \quad d = \frac{a}{2b} + \left(1 - \frac{a^2}{4b}\right)^2. \tag{2.12}$$

The map $\tilde{f}$ is called the *dual* of f and has the form

$$\tilde{f}(x) = 1 + \tilde{a}x^2 + \tilde{b}x^4,$$

with

$$\tilde{a} = (4b - a^2)[8ab + (4b - a^2)^2]/32b^2,$$
$$\tilde{b} = [8ab + (4b - a^2)^2]^3/(8b)^4. \tag{2.13}$$

Duality is reciprocal, $(\tilde{\tilde{f}}) = f$. All of the topological correspondences mentioned after (2.4) hold between f and its dual. For example, if f has an n cycle using the point x, then $\tilde{f}$ has a corresponding n cycle using the point

$$\tilde{x} = h^{-1}(d) \circ G_2(x) = \left(\frac{a}{2b} + x^2\right)\Big/ d. \tag{2.14}$$

In particular, it follows from (2.14) that, if f has an n cycle using a side extremum ($x_\pm = \pm\sqrt{-a/2b}$, $ab < 0$), then the corresponding n cycle of $\tilde{f}$ uses the central extremum ($\tilde{x}_\pm = 0$) and, conversely,[17] if the n cycle of f uses the central extremum $x_0 = 0$, then that of $\tilde{f}$ uses one of the side extrema [$\tilde{x}_0 = \pm(-\tilde{a}/2\tilde{b})^{1/2}$].

The duality relations (2.13) will be useful in Secs. II C and II D below. The points on the curve

$$8ab + (4b - a^2)^2 = 0 \tag{2.15}$$

are all the dual to the origin. Remaining a axis points ($b = 0$, $a \neq 0$) map to infinity under duality, while remaining b-axis points ($a = 0, b \neq 0$) map to the parabola $b = a^2/4$. In addition, there is a line of self-duality, $(\tilde{a}, \tilde{b}) = (a, b)$, which can be parmet-

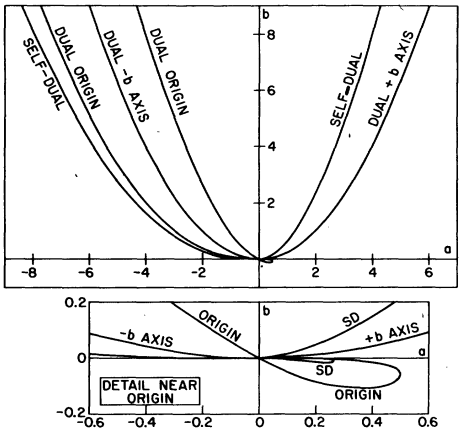

FIG. 3. Mapping of special lines under duality (2.13). The origin maps to the line (2.15). The b axis maps to the parabola $b=a^2/4$. Both the self-dual line and the inverse origin have branches in quadrant IV, as shown in the detail.

rized as

$$a=2c^2(1+c),\quad b=c^3(1+c)^3, \tag{2.16}$$

corresponding to

$$f=h_S^{-1}(1+c)\circ g^{(2)}\circ h_S(1+c), \tag{2.17}$$

with

$$g(x)=1+cx^2.$$

These special lines are shown in Fig. 3. The mapping under duality of some sample regions of the a,b plane is shown in Fig. 4. Notice that regions $\tilde{A}$ and C of Fig. 4 are adjacent, while their duals A and $\tilde{C}$ meet only at the origin. A similar

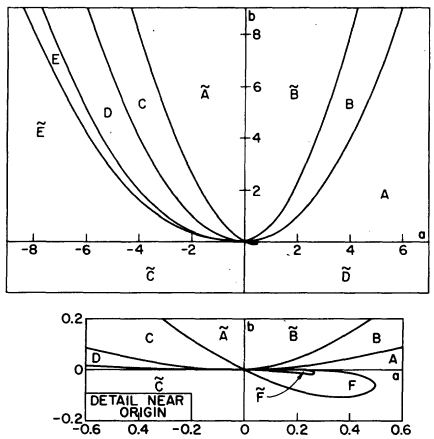

FIG. 4. Mapping of various regions under duality. Region A is the dual of region $\tilde{A}$, etc. Regions that are contiguous across the dual-origin line (2.15) do not remain so under duality.

remark applies to D and E and their duals $\tilde{D}$ and $\tilde{E}$. This occurs because the origin is the dual image of the entire line (2.15).

The iterative behavior of f is completely known along the self-dual line, since $g(x)$ in (2.17) is the well-studied[1] quadratic map (1.2). The map f is iteratively stable for all $-2\leq c\leq\frac{1}{4}$ and otherwise unstable. At c values for which g has a stable $2n$ cycle, $x_1,x_2,\ldots,x_{2n}$, f has two stable n cycles $x_1,x_3,\ldots$ and $x_2,x_4,\ldots$, and is, therefore, bimodal. At c values for which g has a stable $(2n+1)$-cycle, f has a stable $(2n+1)$ cycle and is unimodal. The main bifurcation sequence of g ends at[1] $c=-1.401\,16\ldots$, which translates into $(a,b)=(-1.575\,13,\ 0.177\,58)$.

C. Stable, superstable, and doubly stable n cycles (Ref. 15)

It is straightforward to solve the n-cycle condition (2.1) numerically and then to check stability (2.2). The condition (2.3) for a superstable n cycle requires that one or more of the points $x_1,x_2,\ldots,x_n$ of the cycle be an extremum of f. The central extremum $x_0\equiv 0$ may always appear; however, at most one of the two side extrema can appear in any given cycle, since the evenness of f guarantees that the itineraries of $x_\pm=\pm\sqrt{-a/2b}$ $(ab<0)$ coincide after one step. Thus, each superstable cycle can be classified +, −, 0, 0+, or 0−, according as it uses the indicated extrema. The last two cases denote n cycles $(n\geq 2)$ which use both the central extremum and one side extremum and are, therefore, *doubly stable*. Doubly stable cycles are, indeed, particularly stable. When (1.4) has more than one extremum, all are quadratic. Thus, if x is a member of a doubly stable m cycle,

$$f^{(m)}(x+\delta x)=x+O(\delta x^n),\quad n=4 \tag{2.18}$$

instead of $n=2$ (ordinary superstable cycle). The argument following (2.14) shows that the dual of a doubly stable cycle is also doubly stable, provided only that the dual points $\tilde{x}_0$ and $\tilde{x}_\pm$ are distinct. The exceptional case, $\tilde{x}_0=\tilde{x}_\pm=0$, occurs only for $\tilde{a}=0$, i.e., for

$$\tilde{f}(x)=1+\tilde{b}x^4, \tag{2.19}$$

in which case $\tilde{f}$ has a single *quartic* extremum. Any cycle which uses this quartic extremum satisfies (2.18) and will also be called doubly stable.

Suppose that for a particular set of parameters (a_0,b_0) f has a doubly stable cycle. It is clear that itineraries belonging to all points x sufficiently close to any of the extrema x_0, $x_\pm$ are attracted to such a cycle. It turns out empirically (see Sec. II D) that f is always unimodal. If f is doubly stable for (a_0,b_0), then f is unimodal for (a,b) in

some neighborhood of (a_0, b_0). Doubly stable points will play an important role in the tricritical behavior which terminates the Feigenbaum critical line.

We illustrate some of these notations by simple examples. Regions of stable and superstable fixed points (1 cycles) are displayed in Figs. 5 and 6. Since $f(0)=1$ by our choice of normalization (1.4), superstable fixed points can only occur for (a,b) values such that

$$x_+(a,b)\equiv x_+=f(x_+) \quad \text{or} \quad x_-(a,b)\equiv x_-=f(x_-)\,, \tag{2.20}$$

and the various branches of the curve in Fig. 5 have been labeled accordingly. The condition (2.20) reduces to (2.15). This is not an accident: Had we chosen the more general normalization (2.7), the condition for a superstable fixed point associated with the central peak would have been $C=0$, which via (2.8) is topologically conjugate to $a=b=0$. The discussion following (2.14) then shows that the $x_\pm$ superstable fixed points must occur for (a,b) dual to $(0,0)$.

The regions of fixed-point stability shown in Figs. 5 and 6 contain the superstable line and are bounded [see (2.2)] by curves determined from

$$x_1(a,b)=x_1=f(x_1)\,,$$

with (2.21)

$$f'(x_1)\equiv\left.\frac{df}{dx}\right|_{x=x_1}=\pm 1\,.$$

Over most of the 1-cycle region, f has only one stable fixed point[18]; however, there is a narrow region visible in Fig. 6 in which there are two independent stable fixed points. A typical example of this behavior is shown in Fig. 7: The domains of attraction of the two stable fixed points are disjoint and, between them, exhaust the iterative domain of f (except, of course, for a set of measure zero, the unstable fixed points). The map f is, therefore, bimodal.

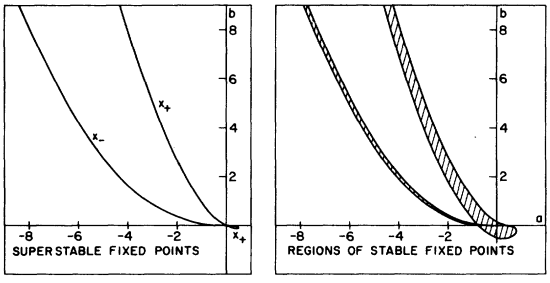

FIG. 5. Loci of stable and superstable fixed points in the a,b plane. The superstable locus coincides with the dual-origin curve of Fig. 3 and its branches have been labeled x_+ or x_- according to the associated extremum. The (cross-hatched) region of fixed-point stability includes the superstable locus. The upper edge of the stable region corresponds to the tangency conditions plotted in Fig. 1.

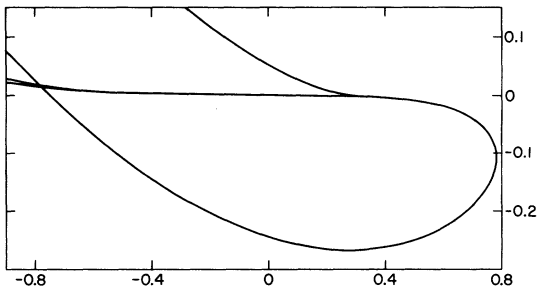

FIG. 6. Detail of the stable fixed-point region shown in Fig. 5. In the very narrow region of intersection of the two branches of stability the function $f(x)$ has two independent stable fixed points.

The superstable 2 cycles are shown in Fig. 8. The x_0 superstable 2 cycle satisfies

$$0=x_0=f^{(2)}(x_0)=f^{(2)}(0)=1+a+b\,. \tag{2.22}$$

The $x_\pm$ superstable 2 cycles can be found in analogy with (2.20); however, it is much easier to invoke duality and simply compute the dual of (2.22).

Intersections of superstable n cycle curves (e.g., Fig. 8) require comment. The set of curves belonging to a single extremum cannot intersect except at the origin. Similarly, curves belonging to x_+ cannot intersect those belonging to x_-, since x_+ and x_- have the same itinerary after one step. x_0 curves can intersect $x_\pm$ curves, as illustrated by Fig. 8. These intersections are of two quite dif-

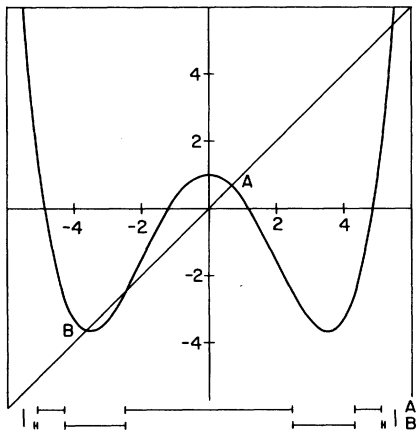

FIG. 7. Iterative plot of the function $f(x)=1-0.75x^2+0.03x^4$. This function has two stable fixed points at $x_A=0.670$ and $x_B=-3.662$. The iterative domain of f is $|x|\leq 5.475$. The domains of attraction of x_A and x_B are indicated below the graph. They exhaust the iterative domain of f (except for a set of measure zero) and interlace with each other as shown.

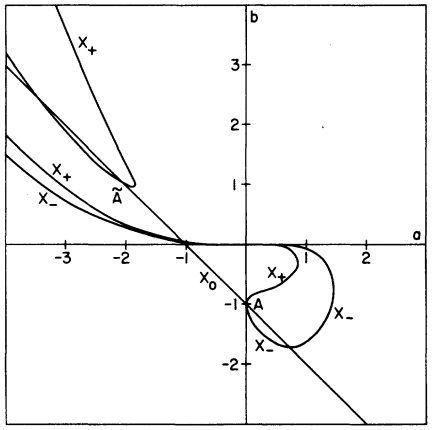

FIG. 8. Superstable 2 cycles. The central-extremum (x_0) curve is just the line $a+b+1=0$. Each branch is labeled according to the peak from which its stability derives. The point A and its dual $\tilde{A}$ are doubly stable. Other intersections are nondynamical.

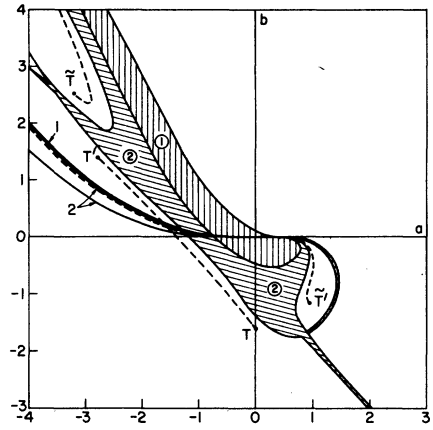

FIG. 10. Nesting regions of 1- and 2-cycle stability. Where such bifurcations proceed to completion, they end in a Feigenbaum critical line. The main critical line TT' and its dual $\tilde{T}\tilde{T}'$ are shown. The normal bifurcation sequence does not occur beyond these tricritical points.

ferent types. At the intersection point there may be two independent superstable cycles, each with its own domain of attraction. At such points f is bimodal and the curves are *dynamically independent*. Alternatively, there may be a single doubly stable cycle at the intersection point. In this case f is unimodal and the curves are *dynamically coupled*. In Fig. 8 only the intersection A and its dual image $\tilde{A}$ are dynamical. The remaining intersections are nondynamical.

Figure 9 shows the regions of stable 2-cycle behavior. Note the bimodal regions surrounding the nondynamical intersections of Fig. 8. The region of 1-cycle stability shown in Fig. 5 nests snugly against the region of 2-cycle stability, as shown in Fig. 10. In particular, following the negative a axis away from the origin, one sees the beginning of the main bifurcation sequence of the quadratic map (1.2). Such sequencing is also seen in other regions of Fig. 10. Whenever such bifurcations run to completion, they terminate in a Feigenbaum critical point. Regions of nesting therefore indicate a Feigenbaum critical line. Note, however, that the complicated topology of the 2-cycle regions already requires that the critical line be broken into segments. We have calculated the position of the main[19] critical lines. They are included for convenience in Fig. 10 and will be discussed in Sec. III.

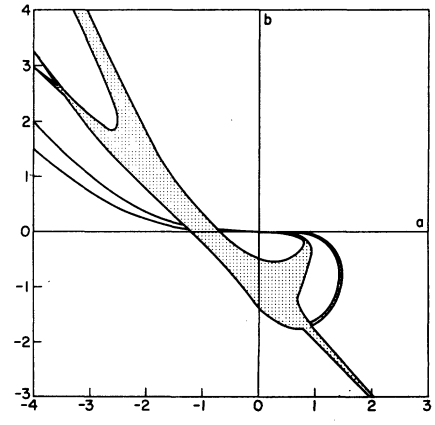

FIG. 9. Regions of stable 2-cycle behavior in the a,b plane.

Figures 11 and 12 show loci of superstable 4 cycles and 3 cycles. Dynamical intersections (which will play a role in Sec. III) are indicated. The general picture which emerges for the central-extremum (x_0) curves is one or more diagonal lines running across the (a,b) plane from upper left to lower right and intersecting the negative a axis at the known values for the simple quadratic map (1.2) and in the standard sequence.[20] (Note that there are two such 4 cycles, one associated with bifurcation of the 2 cycle and the other in the region of inverse bifurcations on the far side of the critical line.) In addition, there are a large number of "fingers" in quadrants II and IV, some very narrow. These poke in towards the origin, cross no axes, and go off to infinity, apparently along the lines $b=0$, $a+b=0$, $a+b+1=0$, and $a+b+2=0$. The $x_\pm$ curves are obtained from the central-extremum curves by duality (2.13). Wherever an x_0 curve crosses (2.15) (see Fig. 3), the corresponding dual passes through the origin, creating the loops visible in quadrant IV.

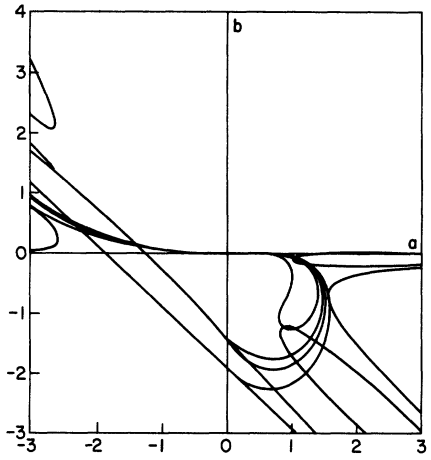

FIG. 11. Superstable 4 cycles. The 4 cycles necessary for the bifurcation sequences leading to TT' and $\tilde{T}\tilde{T}'$ (Fig. 10) is present. Much additional structure is also present. Several of the 4-cycle lines are too narrowly spaced to be resolvable on this graph.

D. Iterative stability

We now return to the question posed in Sec. II A of determining the region of the (a,b) plane over which the function (1.4) is iteratively stable. In principle, this is just the union over n of the regions of stability (see, e.g., Figs. 5 and 9) of all n cycles plus, in addition, those regions where f has no stable n cycles but is iteratively stable by virtue of chaotic itineraries.[21]

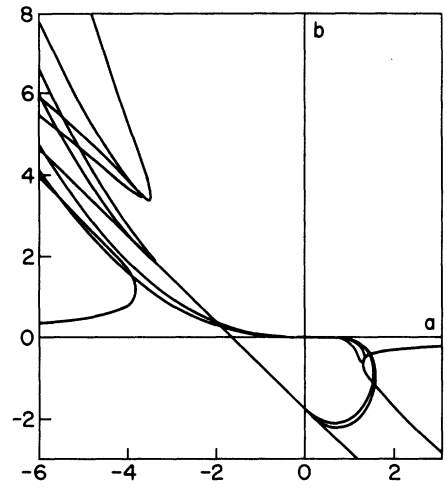

FIG. 12. Superstable 3 cycles. 3 cycles occur in the region beyond the main bifurcation sequence leading to TT' and $\tilde{T}\tilde{T}'$. Otherwise, 3-cycle structure is broadly similar to 2- and 4-cycle structures. Several of the 3-cycle lines are too narrowly spaced to be resolvable on this graph.

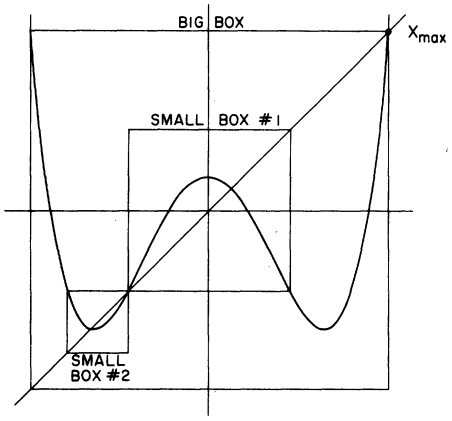

FIG. 13. Illustration of the box construction. A big box and two possible small boxes are shown. If the function remains inside any one (or more) of the boxes over the appropriate domain, then it is guaranteed to be iteratively stable.

Maps of the types I_0 and II_0 (see Figs. 1 and 2), for which there are no solutions of $x=f(x)$, have unbounded itineraries for all x. Their iterative domain is the empty set and they are iteratively unstable. At the boundary between (I_0+II_0) and (I_2+II_2), $y=f(x)$ is tangent to $y=x$, which is just the condition (2.21) giving the upper edge of the stable 1-cycle region. Just beyond this boundary in (I_2+II_2) there are two fixed points, x_{max} (see Fig. 2) and x_{min}, with $f'(x_{max})>1$ and $f'(x_{min})<1$. If $f'(x_{min})>-1$ (as is true throughout I_2), then any x with $|x|<x_{max}$ flows to x_{min} and any x with $|x|>x_{max}$ has an unbounded itinerary, so f is iteratively stable and unimodal.

In other regions of the (a,b) plane the situation is more complicated and we must develop a methodology for establishing iterative stability. Figure 13 illustrates one such criterion, which we call the *box construction*. Let $x_{max}=x_{max}(a,b)$ denote the solution of $x=f(x)$ of largest absolute value. Suppose

$$|x_{max}| \geq |f(x)| \ \forall \ |x| \leq |x_{max}| . \tag{2.23}$$

We refer to this as the "big-box" condition. It is easy to see that points with $|x| \leq |x_{max}|$ have bounded itineraries, while those with $|x|>|x_{max}|$ have unbounded itineraries. Similar "small-box" constructions can be done separately for centeral and side extrema, as suggested in Fig. 13. If any or all of the extrema of f are boxable in the above sense, then f is iteratively stable. For example, in quadrant III, where f has a single peak at $x_0=0$, the box condition (2.23) requires

$$|x_{max}| \geq f(0)=1 , \tag{2.24}$$

so the boundary of guaranteed stability is the line

$$-1 = x_{\max} = f(x_{\max}) = f(1) = 1 + a + b ,$$

and (2.24) is equivalent to

$$a + b \geq -2 . \tag{2.25}$$

When two peaks are independently (small-) boxable, then f is at least bimodal. Systematic application of the box conditions to all peaks and over the whole (a,b) plane leads to a region S of guaranteed iterative stability, pictured in Fig. 14. This rather complicated figure goes into itself under duality.

Failure of the box conditions may or may not imply iterative instability. For example, comparison of Figs. 9 and 14 already shows that the region of stable 2 cycles extends beyond the boundary of guaranteed stability into regions $\tilde{D}_1$ and D_1 of quadrants II and IV, respectively. We develop this situation in more detail. The map (1.4) is infinitely differentiable and it is easy to verify that its Schwartzian derivative

$$Sf(x) \equiv \frac{f'''(x)}{f'(x)} - \frac{3}{2}\left(\frac{f''(x)}{f'(x)}\right)^2 \tag{2.26}$$

is everywhere negative. In quadrant III, where f is single peaked, it satisfies the hypotheses of a theorem due to Singer,[2,22] which concludes that any stable n cycle attracts the peak. Thus, when (2.25) is satisfied (i.e., when the peak itinerary is bounded), f has at most a single stable n cycle, while, when (2.25) fails (i.e., when the peak itinerary is unbounded), f has no stable n cycles. In the former case f is iteratively stable and unimodal.[23] In the latter case f is iteratively unstable.[24] Thus, the region $a+b<-2$ of quadrant III and its dual image in quadrant II are iteratively unstable.

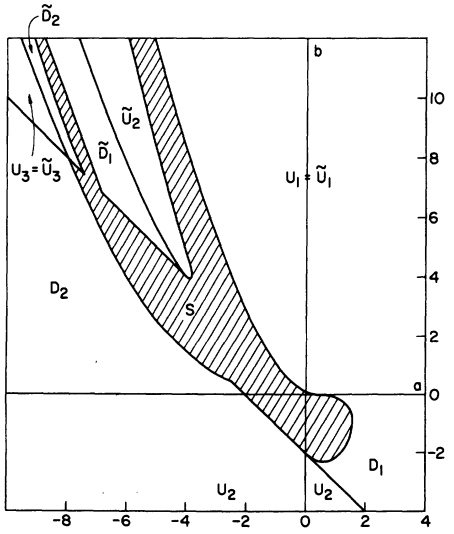

FIG. 14. Iterative stability via the box construction. The cross-hatched region S is guaranteed stable. The regions U and their duals $\tilde{U}$ are guaranteed unstable. Stability of the regions D and their duals $\tilde{D}$ cannot be decided by the simple box construction.

In quadrants II and IV, f has three extrema and does not satisfy the hypotheses of Singer's theorem. We have proceeded empirically. The result of our study may be summarized in a form that applies over the entire (a,b) plane by the following three statements.

(1) When all extrema have unbounded itineraries, then f is iteratively unstable.

(2) When $x_0 = 0$ has a bounded itinerary and $x_\pm$ have an unbounded itinerary or vice versa, then f is iteratively stable and unimodal.

(3) When both x_0 and $x_\pm$ have bounded itineraries, then f is iteratively stable. If the two itineraries are asymptotically distinct, then f is bimodal; if they are asymptotically convergent, then f is unimodal.

If all extrema lie outside the big box of Fig. 13, then statement (1) applies and f is iteratively unstable. Such regions have been indicated U (unstable) in Fig. 14. If all extrema lie inside the big box of Fig. 13, then statement (3) applies and f is iteratively stable. If the central extremum lies outside the big box and the $x_\pm$ extrema lie inside or vice versa, then there are two possibilities: If an inside extremum is small-boxable, then f is stable and unimodal [statement (2)], if not, then the situation remains in doubt. These doubtful regions are denoted D in Fig. 14. We investigated them numerically by the following method: We fix (a,b) and follow the itinerary of the "inside" extremum for 32 steps. If the itinerary ever reaches the region $|x| > |x_{\max}(a,b)|$, then it is unbounded and f is iteratively unstable. If the itinerary remains within the range $-|x_{\max}| < x < |x_{\max}|$, then we declare it bounded (for practical purposes) and f is iteratively stable and unimodal. In practice, the distinction is sharp. Figure 15 shows the results of a scan in (a,b) in region D_1 at a grid interval of 0.015. Similar structure occurs in the other D regions. What appears is a complex set of spines or *spicules* radiating outward from the known-stable region S. The major spicules are readily identifiable with low-n regions of n-cycle stability, which we have seen in Figs. 9, 12, and 13. Many other spicules certainly exist in these regions, however, they become rapidly more narrow as n increases and slip between the mesh of our grid scan. Well-defined regions of entirely unstable behavior are also suggested by Fig. 15. The boundary between

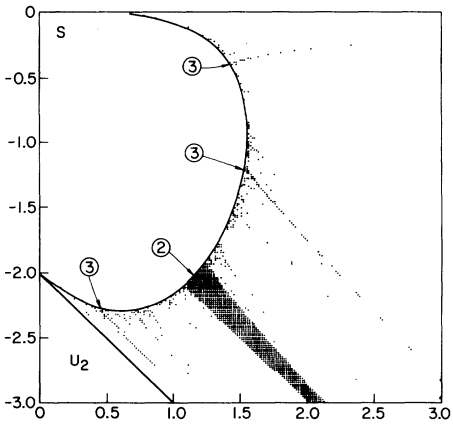

FIG. 15. Iterative stability in the doubtful region D_1 of Fig. 14. Regions S and U_2 are guaranteed stable and unstable, respectively, by the box construction. Points shown were determined iteratively stable by a 200×200 scan, as described in the text. The major spicules are readily identifiable with low-n ($n=2,3$) n cycles, as indicated.

stable and unstable regions appears to be very irregular and may have some fractal character. All the above considerations could be further refined by studying box constructions for the functions $f^{(n)}$ for $n>1$.

III. CRITICAL AND TRICRITICAL BEHAVIOR

A. The Feigenbaum critical line and its dual

The nesting 1- and 2-cycle regions shown in Fig. 10 are the first stages of a standard bifurcation cascade, $1,2,4,8,\ldots$. When this cascade proceeds smoothly to completion, it terminates at a locus of accumulation points, which we shall call a critical line.[4] We already know two points on the critical line: $(a,b)=(-1.401\,16,0)$ on the negative-a (logistic) axis and the intersection of the critical line and the self-dual line given at the end of Sec. II B. There is no difficulty in finding the rest of the critical line numerically. The most efficient method is simply to plot the appropriate loci of central-peak superstable 4 cycles (Fig. 11), 8 cycles, etc., which rapidly converge to the Feigenbaum critical line TT', $a_c=a_c(b)$ [or $b_c=b_c(a)$], shown in Fig. 10. Approaching this line from the upper right always leads through the standard cascade; continuing beyond to the lower left reveals the usual sequence of inverse-bifurcation bands. Asymptotically close to the critical line the position of the superstable 2^n cycles (or any other reference feature one cares to choose) varies [c.f. (1.3)] as

$$a_n(b)=a_c(b)+A(b)/\delta_F^n$$

or

$$b_n(a)=b_c(a)+C(a)/\delta_F^n, \tag{3.1}$$

where the critical amplitudes $A(b)$ or $C(a)$ vary smoothly along the critical line but δ_F is universal.

The new feature here is the fact that the critical line terminates at the special points

$$T=(0,\ -1.594\,90),\quad T'=(-2.814\,03,\ 1.407\,01), \tag{3.2}$$

which we shall refer to as *tricritical points* in analogy to the theory of thermodynamic phase transitions.[25] The mechanism for the termination is the existence of new n-cycle structures which pinch off the orderly sequencing characteristic of the critical line. A variety of interrelated structures exist, which we shall study in more detail in Sec. III C. For the moment we mention three such structures: (i) A tricritical point is the limit of a sequence of doubly stable 2^n-cycle points. For example, the points T and T' are the limit of the dynamically coupled points listed in Table I, the first two of which are visible in Figs. 8 and 11. (ii) A tricritical point is the limit of a sequence of dynamically independent 2^n-cycle intersections (the first few are also visible in Figs. 8 and 11). As a consequence of (i) and (ii) any neighborhood of a tricritical point contains an infinite sequence of interlaced unimodal regions (associated with the doubly stable points) and bimodal regions (associated with the dynamically independent intersections). (iii) Finally, a tricritical point is also characterized as a point at which the critical line is pinched off by a sequence of narrow fingers (see the end of Sec. II C) of high-order out-of-order 2^n cycles. Such a finger is already visible in the 4 cycles (Fig. 8) in quadrant IV, where it is still well away from T [the finger tip only reaches (0.80, −1.25); however, the corresponding 32-cycle finger reaches (0.03, −1.62) and higher-order cycles close in rapidly].

Thanks to Feigenbaum[3] we know that the critical

TABLE I. Sequences of doubly stable 2^n-cycle points (a,b) converging to the tricritical points T and T', which terminate the Feigenbaum critical line. The corresponding points for $\tilde{T}$ and $\tilde{T}'$ may be obtained by using the duality relations (2.13).

Cycle	T	T'
2	(0, −1)	(−2, 1)
4	(0, −1.503 93)	(−2.685 16, 1.342 51)
8	(0, −1.582 25)	(−2.795 75, 1.397 88)
16	(0, −1.593 16)	(−2.811 50, 1.405 75)
32	(0, −1.594 66)	(−2.813 69, 1.406 84)
∞	(0, −1.594 90)	(−2.814 03, 1.407 01)

line is associated with a fixed point of the functional recursion relation,

$$f_{n+1}(x)=\frac{1}{f_n(1)}f_n^{(2)}(xf_n(1)),$$

i.e.,

$$f_{n+1}=h_S^{-1}(f_n(1))\circ f_n^{(2)}\circ h_S(f_n(1)). \tag{3.3}$$

The factor $f_n(1)$ in (3.3) is chosen to preserve normalization, $f_{n+1}(0)=1$ provided $f_n(0)=1$. At any fixed point of (3.3) (and, as we shall see, there are many),

$$f^*=h_S(\alpha)\circ f^{*(2)}\circ h_S^{-1}(\alpha), \tag{3.4}$$

with

$$\alpha=1/f^*(1), \tag{3.5}$$

i.e., f^* is topologically conjugate to $f^{*(2)}$ under rescaling by *magnification factor* α. The mapping (3.4) takes a function $f_n=f^*+\delta f$ near f^* into another function $f_{n+1}=f^*+\delta f'$ near f^*, with

$$\delta f'=\mathfrak{L}(\delta f)+O(\delta f^2), \tag{3.6}$$

where $\mathfrak{L}$ is linear. The eigenvalues Λ_m and eigenvectors e_m of $\mathfrak{L}$ satisfy

$$\mathfrak{L}(e_m)=\Lambda_m e_m \tag{3.7}$$

and provide a convenient basis for describing the region of function space near f^*. For example, if

$$\delta f=\sum_m a_m e_m \tag{3.8}$$

for some set of coefficients a_m, then

$$\delta f'=\sum_m a_m\Lambda_m e_m. \tag{3.9}$$

The fixed point (3.4) of (3.3) associated with the Feigenbaum critical line has the form[3]

$$f_F^*(x)=1+c_2^{(F)}x^2+c_4^{(F)}x^4+\cdots, \tag{3.10}$$

with

$$c_2^{(F)}=-1.5276,\quad c_4^{(F)}=0.1048,\ldots,$$

and

$$\alpha_F=2.502\,91. \tag{3.11}$$

There is only one "relevant"[26] eigenvalue $\Lambda_1\equiv\delta_F=4.669\,20$. All other eigenvalues are "irrelevant," $|\Lambda_m|<1$ for $m>1$, so the corresponding perturbations (3.8) shrink under iteration. The fixed point f_F^* therefore has an inflowing *critical hypersurface* of *codimension* one. The Feigenbaum critical line is the intersection of this critical hypersurface with the a,b plane. Any function f_c on the Feigenbaum critical line (but excluding the endpoints T and T') flows to f_F^* under iteration (3.3). [Nearby functions flow near to f_F^*, through the linear region (3.8), (3.9), and then (3.1) follows.] In particular, if $f_0(x)\equiv f(x)$, then iteration under (3.3) gives

$$f_n=h_S^{-1}(f^{(2^n)}(0))\circ f^{(2^n)}\circ h_S(f^{(2^n)}(0)), \tag{3.12}$$

with

$$f^{(2^n)}(0)=\prod_{m=1}^{n-1}f_m(1). \tag{3.13}$$

So, if f_c is on the Feigenbaum critical line, then

$$\lim_{n\to\infty}(f_c)_n=f_F^*. \tag{3.14}$$

Equation (3.14) is, in fact, a convenient way of finding the fixed-point function f_F^*. In addition, putting $x=1$ in (3.14) and using (3.12) and the definition (3.5) of the magnification factor, we find

$$\alpha_F=\lim_{n\to\infty}[f_c^{(2^n)}(0)/f_c^{(2^{n+1})}(0)], \tag{3.15}$$

which is numerically convenient.

The dual of the Feigenbaum critical line TT' is another critical line $\tilde{T}\tilde{T}'$, shown in Fig. 10. Endpoints of this dual line are tricritical points located dual to (3.2),

$$\begin{aligned}\tilde{T}&=(-3.189\,80,\ 2.543\,71),\\ \tilde{T}'&=(0.955\,61,\ -1.149\,81).\end{aligned} \tag{3.16}$$

The dual critical line passes through (0, 0) because TT' crosses (2.15) and through infinity because TT' crosses the a axis. The critical lines TT' and $\tilde{T}\tilde{T}'$ intersect at the self-dual line; however, they are dynamically independent: Feigenbaum critical behavior uses the central extremum, while its dual uses the $x_\pm$ extrema, in accordance with the discussion after (2.14). The continuity of the duality relations (2.13) guarantees that (3.1) holds in the vicinity of the dual critical line. Does the dual line lie on the critical hypersurface of the fixed point f_F^*? The answer is no. Indeed, the iteration procedure (3.2)–(3.4) does not even lead to a function with finite coefficients like (3.10). The reason is simple enough. The 2^n cycles in the bifurcation behavior of $\tilde{T}\tilde{T}'$ use one of the side extrema $x_\pm$ instead of the central extremum. However, the iteration (3.3) continually magnifies the function around the origin, pushing the active part of the function near the $x_\pm$ extrema off to infinity. To achieve a finite fixed point, it would be necessary to translate the active peak to the origin before applying (3.3), (3.12), and (3.14). The infinite fixed point which controls $\tilde{T}\tilde{T}'$ is topologically conjugate to f_F^* in this sense.

B. Tricriticality: Exponents

The tricritical point T is located as the limit of the set of doubly stable 2^n cycles situated on the

negative-b axis. Locating T' would appear to require a two-dimensional search. Luckily, this is not so, as we now explain. For each $n>1$ there are several doubly stable points in quadrant II (see Sec. III D). Each such cycle uses the extrema x_0 and x_+; however, the different doubly stable points use them in different orders. The sequence of doubly stable 2^n cycles which converges to T' turns out to use the two extrema in the order x_0, $x_+,\ldots$. Normalization requires $f(x_0)=f(0)=1=x_+(a,b)$, so $a=-2b$, as exemplified in Table I. Thus, the doubly stable points leading to T' all lie on the line

$$f(x)=1-2cx^2+cx^4 \tag{3.17}$$

and can be found by a one-dimensional search.

We turn now to tricritical behavior and start with an analysis of the point T. Functions on the b axis have the form

$$f(x)=1+bx^4 \tag{3.18}$$

and are iteratively stable and unimodal for $-2\leq b\leq \frac{27}{256}$. The iterative behavior of such functions as b travels down the negative-b axis is entirely similar to that of the functions (1.2): There is a main bifurcation sequence (the beginnings of which we have already seen in Figs. 10 and 11 and Table I), which has its limit at $b_T=-1.594\,901\,356\,228\,8\ldots$. For $-2<b<b_T$ there is a corresponding sequence of inverse-bifurcation bands. The vicinity of b_T is characterized by scaling behavior. For example, the positions b_n of the doubly stable 2^n cycles for $b>b_T$ and large n vary as

$$b_n-b_T=B/(\delta_T^{(1)})^n\ , \tag{3.19}$$

with $\delta_T^{(1)}=7.284\,69$ and $B=4.888$, in precise parallelism to (1.3). The number $\delta_T^{(1)}$ differs from δ_F because (3.18) has a quartic rather than quadratic maximum[5] but is otherwise universal in the same sense. The amplitude B is nonuniversal.

The origin of the scaling behavior (3.19) is the existence of a new fixed point of (3.3), which we denote [cf. (3.10)]

$$f_T^*(x)=1+c_4^{(T)}x^4+c_8^{(T)}x^8+\cdots\ , \tag{3.20}$$

where f_T^* satisfies (3.4) with magnification factor

$$\alpha_T=1/f_T^*(1)=(1+c_4^{(T)}+c_8^{(T)}+\cdots)^{-1}\ . \tag{3.21}$$

There are several ways of finding the tricritical fixed-point function.[27] One of the simplest ways follows the logic of (3.12)–(3.15): when $b=b_T$, $f(x)=f_T(x)\equiv 1+b_Tx^4$. Then

$$f_T^*=\lim_{n\to\infty}(f_T)_n \tag{3.22}$$

and

$$\alpha_T=\lim_{n\to\infty}[f_T^{(2^n)}(0)/f_T^{(2^{n+1})}(0)]\ . \tag{3.23}$$

Equation (3.22) can be used to find the coefficients $c_{4n}^{(T)}$ as follows: Let

$$f_T^{(n)}(x)=f_T^{(n)}(0)+C_4^{(n)}x^4+\cdots\ , \tag{3.24}$$

then it is easy to develop the recursion relation,

$$C_4^{(n+1)}=4b_T[f_T^{(n)}(0)]^3C_4^{(n)}\ . \tag{3.25}$$

However, $C_4^{(1)}=b_T$, so

$$C_4^{(n)}=\tfrac{1}{4}(4b_T)^{2^n}\prod_{m=1}^{2^n-1}[f_T^{(m)}(0)]^3\ ,$$

and inclusion of the additional factors in (3.12) yields

$$c_4^{(T)}=\lim_{n\to\infty}\tfrac{1}{4}(4b)^{2^n}\prod_{m=1}^{2^n}[f_T^{(m)}(0)]^3\ . \tag{3.26}$$

Derivation of similar expressions for higher-order coefficients is straightforward. We find from (3.23)

$$\alpha_T=-1.690\,30\ldots\ . \tag{3.27}$$

Results for $C_{4n}^{(T)}$ are given in Table II.

Perturbation about the fixed point (3.20) determines scaling behavior, as outlined in Sec. III A. There are two types of perturbations, $\delta f=\delta f^{(e)}+\delta f^{(o)}$, with

$$\delta f^{(e)}=a_4x^4+a_8x^8+\cdots \tag{3.28}$$

and

$$\delta f^{(o)}=a_2x^2+a_6x^6+\cdots\ , \tag{3.29}$$

involving powers x^{2k} with even or odd k, respectively. Because f_T^* is a polynomial in x^4, the iteration of an even δf cannot generate any odd component. Hence, in terms of $\delta f\equiv\binom{\delta f^{(e)}}{\delta f^{(o)}}$, we have

$$\begin{pmatrix}\delta f'^{(e)}\\ \delta f'^{(o)}\end{pmatrix}=\mathfrak{L}(\delta f)=\begin{pmatrix}* & *\\ 0 & *\end{pmatrix}\begin{pmatrix}\delta f^{(e)}\\ \delta f^{(o)}\end{pmatrix}.$$

TABLE II. Coefficients of the tricritical fixed-point function $f_T^*(x)=1+c_4^{(T)}x^4+c_8^{(T)}x^8+\ldots$. These coefficients were obtained via (3.26) and its higher-order analogs. Note that the sum rule (3.21) is well satisfied.

$c_4^{(T)}$	$-1.834\,11$
$c_8^{(T)}$	$0.012\,96$
$c_{12}^{(T)}$	$0.311\,90$
$c_{16}^{(T)}$	$-0.062\,02$
$c_{20}^{(T)}$	$-0.037\,54$
$c_{24}^{(T)}$	$0.017\,66$

Although $\delta f^{(o)}$ couples to both $\delta f'^{(e)}$ and $\delta f'^{(o)}$, $\delta f^{(e)}$ couples only to $\delta f'^{(e)}$. The reducibility of (δf) into a semiblock form implies that the eigenvalue problems (3.7) for the even and odd perturbations do not mix and may be considered independently. Both even and odd subspaces have, of course, an infinite number of eigenvalues and eigenvectors; however, in each case only one eigenvalue is relevant ($|\Lambda|>1$) and the rest are irrelevant ($|\Lambda|<1$). The largest even eigenvalue controls flows in the b (x^4) direction near tricriticality and is just the universal number $\delta_T^{(1)}$ introduced in (3.19) and determined numerically from superstable 2^n-cycle spacings. Finding it and the other even eigenvalues by solving (3.7) with (3.28) is feasible but uninteresting. The largest odd eigenvalues we denote $\delta_T^{(2)}$. We shall show below that $\delta_T^{(2)}$ is simply related to the magnification factor

$$\delta_T^{(2)}=\alpha_T^2=2.85713, \tag{3.30}$$

and that the irrelevant odd eigenvalues are just the inverse odd powers of (3.30), $(\delta_T^{(2)})^{-(2n+1)}$. To see this, take $f_n=f_T^*+\delta f$ and iterate (3.3) once to get

$$f_{n+1}(x)=f_T^*(x)+\delta f'(x)$$
$$=\frac{1}{f_n(1)}\left[f_T^{*(2)}(xf_n(1))+\delta f(xf_n(1))f_T^{*\prime}(f_T^*(xf_n(1)))+\delta f(f_T^*(x(f_n(1))))\right]+O(\delta f^2). \tag{3.31}$$

The first and third terms in the brackets are always even; only the second term can be odd. As we mentioned earlier, we only need to work in the odd k space to obtain the desired eigenvalue. Thus, to linear order, we have

$$\delta f^{(o)\prime}(x)=a_2'x^2+a_6'x^6+\cdots$$
$$=\frac{1}{f_T^*(1)}f_T^{*\prime}(f_T^*(xf_T^*(1)))\delta f^{(o)}(xf_T^*(1)). \tag{3.32}$$

Equation (3.32) has the structure

$$a_k'=\sum_l M_{kl}(\{c^{(T)}\})a_l,\quad k,l=2,6,10,\ldots. \tag{3.33}$$

The eigenvalues of M are the odd eigenvalues of (3.7). Because the coefficient of $\delta f^{(o)}$ in (3.32) is a polynomial in x^4, a_k' cannot depend on a_l for $l>k$, so M is triangular and its eigenvalues are simply M_{kk}. To find M_{kk}, we can set $x=0$ in the coefficient of $\delta f^{(o)}$ to get

$$M_{kk}=[f_T^*(1)]^{k-1}f_T^{*\prime}(1). \tag{3.34}$$

However, f_T^* satisfies (3.4),

$$f_T^*(x)=\frac{1}{f_T^*(1)}f_T^{*(2)}(xf_T^*(1)). \tag{3.35}$$

Differentiating (3.35) with respect to x and then letting $x\to 0$ leads to

$$1=f_T^{*\prime}(1)[f_T^*(1)]^3, \tag{3.36}$$

so finally,

$$M_{kk}=[f_T^*(1)]^{k-4}=\alpha_T^{4-k}, \tag{3.37}$$

which gives (3.30) and the irrelevant odd eigenvalues.

Because there are two relevant eigenvalues at the fixed point f_T^*, the tricritical hypersurface, which flows to f_T^* under iteration (3.3), has codimension equal to 2. This hypersurface evidently intersects the a,b plane at T and controls the scaling behavior there (see Sec. III C). It is by no means obvious that the tricritical point T' at the other end of the Feigenbaum line is also on the tricritical hypersurface belonging to f_T^*. We have verified numerically that it is by observing that $\lim_{n\to\infty}(f_{T'})_n=f_T^*$ [via (3.23), (3.26), etc.]. It follows that behavior near T' is described by the eigenvalues $\delta_T^{(1)}$, $\delta_T^{(2)}$, and α_T.

We turn now to the tricritical points terminating the dual critical line $\tilde{T}\tilde{T}'$. Duality guarantees that scaling behavior near $\tilde{T}$ and $\tilde{T}'$ is described by the universal numbers $\delta_T^{(1)}$ and $\delta_T^{(2)}$. It does not follow, however, that $\tilde{T}$ and $\tilde{T}'$ flow to the fixed point f_T^* and, indeed, they do not (cf. the situation with the dual critical line). Direct iteration in analogy to (3.22)–(3.26) shows that $\tilde{T}$ and $\tilde{T}'$ flow to another tricritical fixed point, given by

$$f_{\tilde{T}}^*(x)=[f_T^*(\sqrt{x})]^2, \tag{3.38}$$

with

$$\alpha_{\tilde{T}}=\alpha_T^2. \tag{3.39}$$

Note that (3.38) is just of the form (2.4), with $h(x)=\sqrt{x}$, $h^{-1}(x)=x^2$, and so $f_{\tilde{T}}^*$ is topologically conjugate to f_T^*. These amusing relations are not hard to derive: When applied to points on the b axis, the duality relations (2.10) and (2.11) read

$$G_1(x)=1+bx^2,\quad G_2(x)=x^2, \tag{3.40}$$

so

$$\tilde{f}_T(x)\equiv f_{\tilde{T}}(x)=G_2(G_1(x))=(1+bx^2)^2=[f_T(\sqrt{x})]^2. \tag{3.41}$$

Thus, in analogy with (3.23)

$$\alpha_{\bar{T}} = \lim_{n\to\infty}\left(\frac{f_{\bar{T}}^{(2^n)}(0)}{f_{\bar{T}}^{(2^{n+1})}(0)}\right)$$

$$= \lim_{n\to\infty}\left(\frac{f_T^{(2^n)}(0)}{f_T^{(2^{n+1})}(0)}\right)^2 = \alpha_T^2 . \tag{3.42}$$

Similarly,

$$f_{\bar{T}}^{*} = \lim_{n\to\infty} (f_{\bar{T}})_n , \tag{3.43}$$

and substitution of (3.41) leads to (3.38).

C. Tricritically: Crossover and scaling functions

The tricritical fixed-point discussion of the preceding section sets the stage for an examination of the structure of n cycles, etc. (the phase diagram) near the points T, T', and their duals. It is a property of the iteration (3.3) that, if f_n has an m cycle, $x_1, x_2, \ldots, x_m$, with even m, then f_{n+1} has two $m/2$ cycles, $x_1/f_n(1), x_3/f_n(1), \ldots$, and $x_2/f_n(1), x_4/f_n(1), \ldots$. If the m cycle of f_n is superstable, then both the $m/2$ cycles of f_{n+1} are superstable (f_{n+1} is at least bimodal). If m is odd, the f_{n+1} has an m cycle, $x_1/f_n(1), x_3/f_n(1), \ldots$, $x_2/f_n(1), x_4/f_n(1), \ldots$. Again, f_n superstable implies f_{n+1} superstable.

In the linear region (3.6)–(3.9) near a fixed point, these considerations take a particularly concrete form. Consider, for example, a function f_n with a 2^m cycle which lies near f_T^* but not on the tricritical hypersurface. Such a function has the form

$$f_n = f_T^* + \delta f ,$$

with

$$\delta f(x) = a_1 e_1(x) + a_2 e_2(x) , \tag{3.44}$$

where $e_1(x)$ and $e_2(x)$ are the eigenvectors belonging to $\delta_T^{(1)}$ and $\delta_T^{(2)}$, respectively. The iterate function (which has two 2^{m-1} cycles) is

$$f_{n+1} = f_T^* + \delta f' ,$$

with (3.45)

$$\delta f'(x) = \delta_T^{(1)} a_1 e_1(x) + \delta_T^{(2)} a_2 e_2(x) ,$$

i.e., it has moved away from the tricritical hypersurface by a factor $\delta_T^{(1)}$ in the even subspace and $\delta_T^{(2)}$ in the odd subspace [see (3.28) and (3.29)].

Now, consider the neighborhood of the tricritical point T. Any point in this neighborhood lies near the tricritical hypersurface and therefore maps after a few iterations into the linear neighborhood of f_T^*. It follows that the near neighborhood of T inherits the scaling structure of (3.44) and (3.45), only in variables appropriately skewed by the intervening iterations. These *scaling variables* are a natural set of coordinates near the point T. They may be taken to be

$$u_1 = b - b_T - a\tan\theta , \quad u_2 = a/\cos\theta , \tag{3.46}$$

where the slope of the critical line is

$$\tan\theta = -1.2347 , \tag{3.47}$$

as illustrated in Fig. 16. Cycle structure near T has much regularity, when described in terms of u_1 and u_2. For example, if there is a superstable 2^n cycle at (u_1, u_2), then there is a superstable 2^{n-1} cycle at $(\delta_T^{(1)} u_1, \delta_T^{(2)} u_2)$, a superstable 2^{n-2} cycle at $[(\delta_T^{(1)})^2 u_1, (\delta_T^{(2)})^2 u_2]$, etc. provided only that all coordinates remain small enough so the points have not departed significantly from T (i.e., from the tricritical hypersurface).

These considerations allow a scaling[28] description of the crossover from critical behavior along the Feigenbaum line to tricritical behavior along the b axis (region 2 of the scaling variables in Fig. 16). The position $u_1^{(n)}(u_2)$ of the superstable 2^n cycles in this region has a simple scaling form,

$$(\delta_T^{(1)})^n u_1^{(n)} = \mathcal{F}((\delta_T^{(2)})^n u_2) , \tag{3.48}$$

which is valid with a *single* function $\mathcal{F}$ independent of n, provided $n \gg 1$ and $|u_1|, |u_2| \ll 1$ but for arbitrary values of the scaled combinations $(\delta_T)^n u$. Equation (3.48) must, of course, incorporate the known behavior on the b axis and along the critical line. On the b axis $u_2 = 0$, $u_1 = b - b_T$, so (3.19) gives

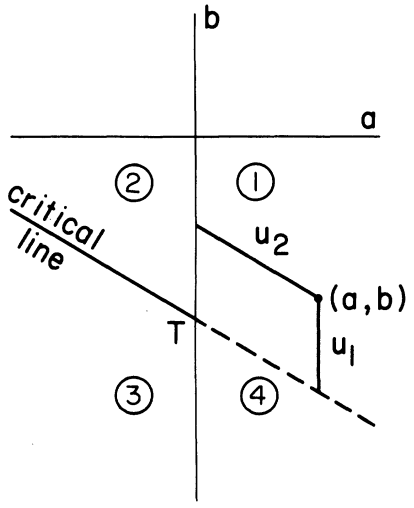

FIG. 16. Scaling variables for the tricritical point T. Equation (3.46) defines scaling variables (u_1, u_2) with reference to the point T, the b axis, and the critical line. In region 2 there is crossover between critical behavior near the critical line and tricritical behavior near the b axis.

$$\mathcal{F}(0)=B. \tag{3.49}$$

On the other hand, at fixed $u_2\neq 0$ (3.48) must agree with (3.1) as $u_1\to 0$, so at large x $\mathcal{F}(x)\sim x^{\gamma}$ and, comparing

$$u_1^{(n)}\sim(\delta_T^{(1)})^{-n}[(\delta_T^{(2)})^n u_2]^{\gamma}\sim C/\delta_F^n, \tag{3.50}$$

we deduce that the critical amplitude $C(a)$ vanishes as $a\to 0$ as a^{γ}, with

$$\gamma=\frac{\ln\delta_T^{(1)}-\ln\delta_F}{\ln\delta_T^{(2)}}=0.4237, \tag{3.51}$$

which we have verified numerically.

Such scaling considerations are not restricted to region 3 (Fig. 16). Indeed, the n-cycle structure in the entire neighborhood of T scales in accordance with the discussion after (3.47). This point is illustrated by Figs. 17–20, which show the structure of 2^n cycles for $n=2$, 3, and 4 displayed in terms of the scaling combinations $(\delta_T^{(1)})^n u_1$ and $(\delta_T^{(2)})^n u_2$. The structure displayed should become fixed as $n\to\infty$. For $n=2$ some nonscaling features are observable far from the origin; however, $n=3$ and $n=4$ are already practically indistinguishable. Note that at fixed $\delta_T^n u$, large n probes small u; thus, Figs. 17–20 illustrate graphically the high-order 2^n-cycle structures which pinch off the critical line at T. A similar discussion of behavior near T', $\bar{T}$, and $\bar{T}'$ could be made.

D. Other tricritical points

In this paper we have confined our discussion to the main Feigenbaum critical line TT' and its dual. We note in closing that tricritical structures exist at many other points in the a,b plane.

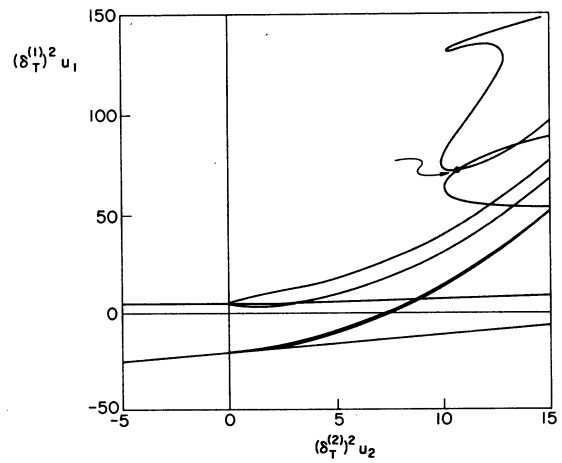

FIG. 17. Superstable 4 cycles near T plotted with scaling variable $u(\delta_T)^2$. Data is the same as Fig. 11. The point marked by the arrow is doubly stable. Nonscaling behavior is observable at the upper right.

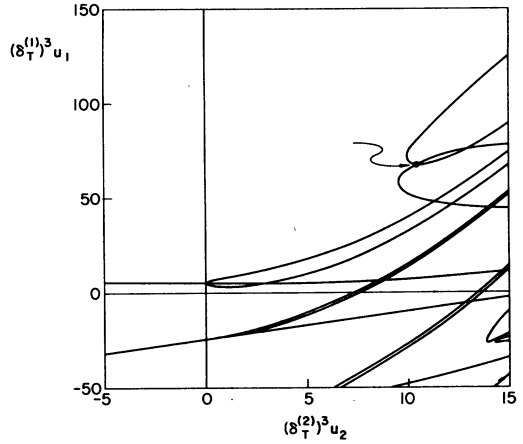

FIG. 18. Superstable 8 cycles near T plotted with scaling variables $u(\delta_T)^3$. The point marked by the arrow is doubly stable. This figure and Fig. 19 coincide except for small numerical differences.

Let us focus on the characterization (Sec. III A) of a tricritical point as the $n\to\infty$ limit of a set of doubly stable 2^n-cycle points. Consider only quadrant IV. The 2 cycles have a single doubly stable point (Fig. 8) at $(0,-1)$. The 4 cycles have (Fig. 11) two such points, $(0,-1.503\,93)$ and $(0.811\,76,-1.239\,53)$. The 8 cycles have four such points, etc. This sequence is illustrated in Fig. 21 through order $n=3$. It appears that, in going from n to $n+1$, each doubly stable point splits, forming as $n\to\infty$ a whole cascade of tricritical points. The outer sequence leads to T and $\bar{T}'$. Others lie between T and $\bar{T}'$. Each limiting point has an infinite number of others in its neighbor-

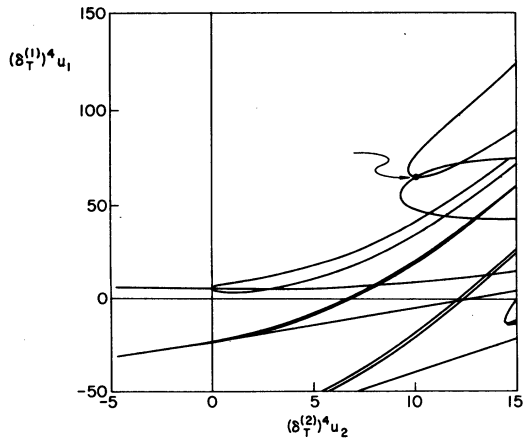

FIG. 19. Superstable 16 cycles near T plotted with scaling variables $u(\delta_T)^4$. The point marked by the arrow is doubly stable. This figure is already an excellent approximation to the exact $n\to\infty$ scaling function in this region of variables.

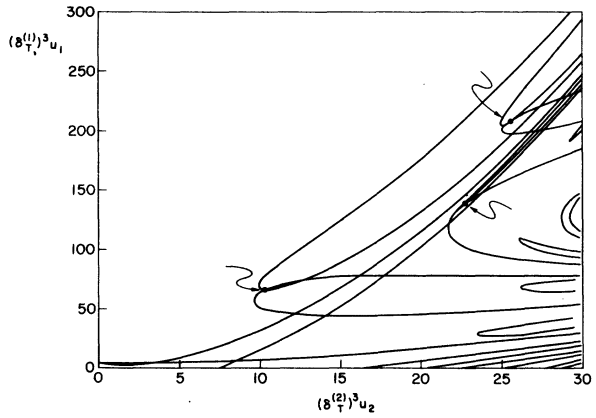

FIG. 20. Superstable 8 cycles associated with the extrema x_0 and x_- (x_+ has been omitted for simplicity). Otherwise, this is the same as Fig. 18 except for the larger scale. Note the additional doubly stable points.

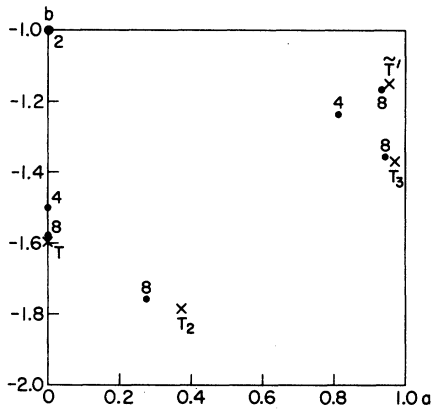

FIG. 21. Doubly stable 2^n cycles in the region between T and $\tilde{T}'$. The points T and $\tilde{T}'$ are marked by crosses. In this region there are one 2 cycle, two 4 cycles, four 8 cycles, etc. All the $n \to \infty$ limit points are presumably tricritical.

hood. Figures 17–19 show two sets of doubly stable 2^n-cycle points converging to T, one on the $u_2 = 0$ (b) axis and the other located at $(\delta_T^{(1)n} u_1, \delta_T^{(2)n} u_2) = (66.4, 10.3)$. Figure 20, which is on a larger scale, shows two additional doubly stable points, and it seems likely that there are many more at larger values of the scaling variables. The self-similarity observable in the scaling plots suggest that the tricritical points may form a Cantor set. At each level of n, we may label a 2^n doubly stable cycle mentioned above as right (R) or left (L) relative to its parent. We can then specify a tricritical point by a sequence of R's and L's. Conversely, any such a R-L sequence specifies a tricritical point. For instance, the tricritical point T is $R^\infty \equiv (R, R, \ldots)$ and the tricritical point $\tilde{T}'$ is L^∞. In Fig. 21, we have also plotted the locations of two additional tricritical points $T_2 = (0.35031, -1.7980)$ and $T_3 = (0.9704, -1.3767)$. In terms of the R-L notation, T_2 is RL^∞ and T_3 is LR^∞. We have not at this stage located the critical lines associated with these tricritical points, nor have we explored the question of what fixed point they flow to under the iteration (3.3). Preliminary evidence shows other doubly stable points for the 8 cycles and above, which may well belong to additional tricritical sequences.

ACKNOWLEDGMENTS

We acknowledge with thanks the useful advice from and conversations with A. E. Jackson, L. P. Kadanoff, P. C. Martin, Y. Oono, and R. L. Schult. We thank L. H. Smith for help with computing. This work was supported in part by the National Science Foundation under Grants Nos. NSF DMR78-21069, NSF PHY79-00272, and by the Office of Naval Research under Contract No. N00014-80-C-0840.

[1]R. M. May, Nature 261, 459 (1976).
[2]P. Collet and J.-P. Eckmann, *Iterated Maps on the Interval as Dynamical Systems* (Birkhäuser, Basel, 1980); both Refs. 1 and 2 contain extensive references.
[3]M. Feigenbaum, J. Statis. Phys. 19, 25 (1978); *ibid.* 21, 669 (1979).
[4]*Phase Transitions and Critical Phenomena*, edited by C. Domb and M. S. Green (Academic, New York, 1976), Vol. 6.
[5]B. Derrida, A. Gervois, and Y. Pomeau, J. Phys. A 12, 269 (1979).
[6]B. Derrida and Y. Pomeau, Phys. Lett. 80A, 217 (1980).
[7]Proceedings of CNLS Conference—Nonlinear Problems: Present and Future (North-Holland, in press).
[8]The relation is $a = \lambda(2-\lambda)/4$, so $\lambda = 1$ (where a fixed point away from $x = 0$ first appears in the logistic map) is equivalent to $a = \frac{1}{4}$, while $\lambda = 4$ (beyond which all of the unit intervals except a set of measure zero maps to $|x| \to \infty$) is equivalent to $a = -2$.
[9]For a study of chaotic transitions and distributions among bands, see S. J. Chang and J. Wright, Phys. Rev. A 23, 1419 (1981).
[10]The S-unimodal maps of Ref. 2.
[11]M. Metropolis, M. L. Stein, and P. R. Stein, J. Combinatorial Theor. 15, 25 (1973).
[12]P. Collet, J.-P. Eckmann, O. E. Lanford III, Commun. Math. Phys. 76, 211 (1980).
[13]Some of the results of this work are reported briefly in a short communication which will appear in Ref. 7:

S. J. Chang, M. Wortis, and J. Wright, Tricritical points and bifurcations in a quartic map (in press).

[14]For our purposes there is no need to distinguish between the ergodic and nonperiodic itineraries of Ref. 2.

[15]One-peak maps with this property are called "most stable" in Ref. 13. In this paper, we follow the convention of Refs. 2 and 5 and refer them as superstable. A cycle is called doubly stable if it is doubly superstable.

[16]The term "unimodal" is used in a similar but more restricted sense in Ref. 2.

[17]The converse is proved as follows: If the n cycle of f uses $x_0 = 0$, then there exists a y_0 such that $x_0 = G_1(G_2(y_0))$. Application of (2.14) to y_0 gives a $\tilde{y}_0$ which is a side extremum of $\tilde{f}$.

[18]A function $f(x)$ in the 1-cycle region may be unimodal or bimodal. As we shall see below, it is quite possible for a stable n cycle to coexist with a stable m cycle ($n = m$ or $n \neq m$) or with chaotic trajectories.

[19]There are many other Feigenbaum critical lines in the phase diagram. The "main" critical lines shown in Fig. 10 have a complete bifurcation sequence 1, 2, 4, 8, ... The other critical lines have truncated sequences 2, 4, 8, ..., 4, 8, 16, ..., and so forth.

[20]Note, for example, that the lower of the two main diagonal 4-cycle lines in Fig. 11 crosses the negative a axis beyond a_c. It corresponds to the "chaotic 4 cycle," which occurs in the region of inverse bifurcation.

[21]If the quadratic map (1.2) is a good guide, then we may expect that the n-cycle regions are dense (Ref. 2), even though the chaotic regions have finite measure [conjectured in Ref. 2, proven by M. Jakobson (unpublished)].

[22]D. Singer, SIAM (J. Appl. Math.) Rev. 35, 260 (1978).

[23]When (2.25) is satisfied in quadrant III, the whole measure of the iterative domain of f is apparently exhausted by either a single stable n cycle or a single region of chaotic itineraries. In principle, there are two additional possibilities: simultaneous existence of two or more distinct chaotic regions or coexistence of one stable n cycle with one or more distinct chaotic regions. These possibilities do not seem to occur in practice; however, to the best of our knowledge they have not been rigorously ruled out, even for the logistic map.

[24]Again, there exists the logical possibility that f possesses some nonzero region of chaotic itineraries. So far as we know this does not occur; however, we are aware of no rigorous argument to exclude it.

[25]In the theory of phase transitions a tricritical point marks the point where a line of second-order transitions (a critical line) becomes first order. It is characterized by the appearance of a new fixed point with an extra relevant variable. See R. B. Griffiths, Phys. Rev. Lett. 24, 715 (1970); E. K. Riedel, *ibid.* 28, 675 (1972); E. K. Riedel and F. J. Wegner, *ibid.* 29, 349 (1972). Let the reader be warned, however, that the parallel is imperfect: What happens in the bifurcation problem beyond the tricritical point is not analogous to first-order behavior. Furthermore, there is not here (as there would be in the phase-transition problem) an enlarged parameter space containing three critical lines and a triple line meeting at tricriticality.

[26]We follow here the phase-transition terminology of, for example, Ref. 4.

[27]One method (Ref. 3) is to substitute (3.20) into the fixed-point equation (3.4) and then truncate to some given order. A simple two-coefficient truncation gives $c_4^{(T)} = -1.855$, $c_8^{(T)} = 0.278$, and $\delta_T^{(1)} = 8.33$, in reasonable agreement with the accurate results (3.19) and Table II.

[28]An early example of this method was the analysis by J. T. Ho and J. D. Litster, Phys. Rev. Lett. 22, 603 (1969), of the magnetic equation of state of $CrBr_3$.